doi:10.1038/nature11943

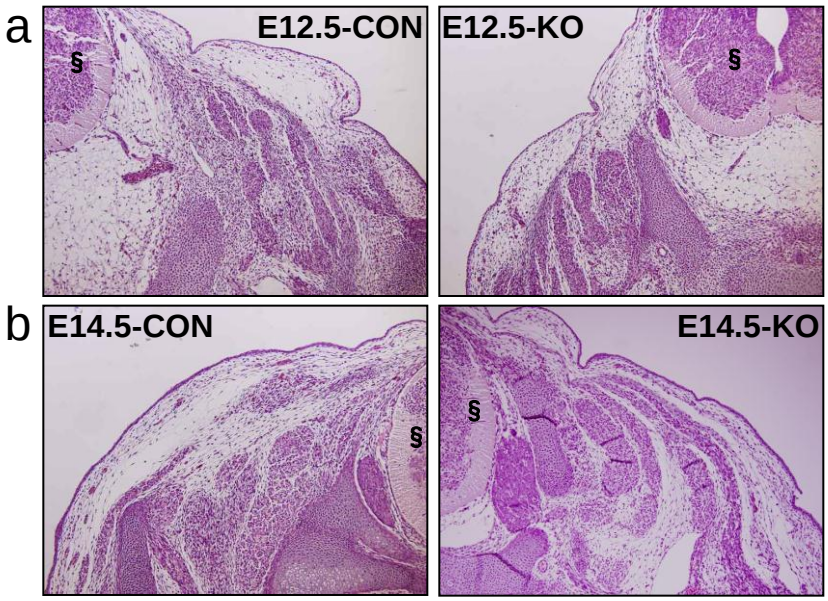

Supplementary Figure S1

Loss of *Bmpr1a* in the Myf5^{+} lineage does not result in obvious morphological changes prior to E16.5.

a, **b**, Haematoxylin & Eosin staining of sections of the interscapular areas of mouse embryos at embryonic stages E12.5 and E14.5. Transversal sections of the same anatomical location were prepared for control (CON, left panel) and Myf5-BMPR1A-KO mice (KO, right panel). Photographs (100x original magnification) of the scapular region were acquired (§ indicates location of the spinal cord).

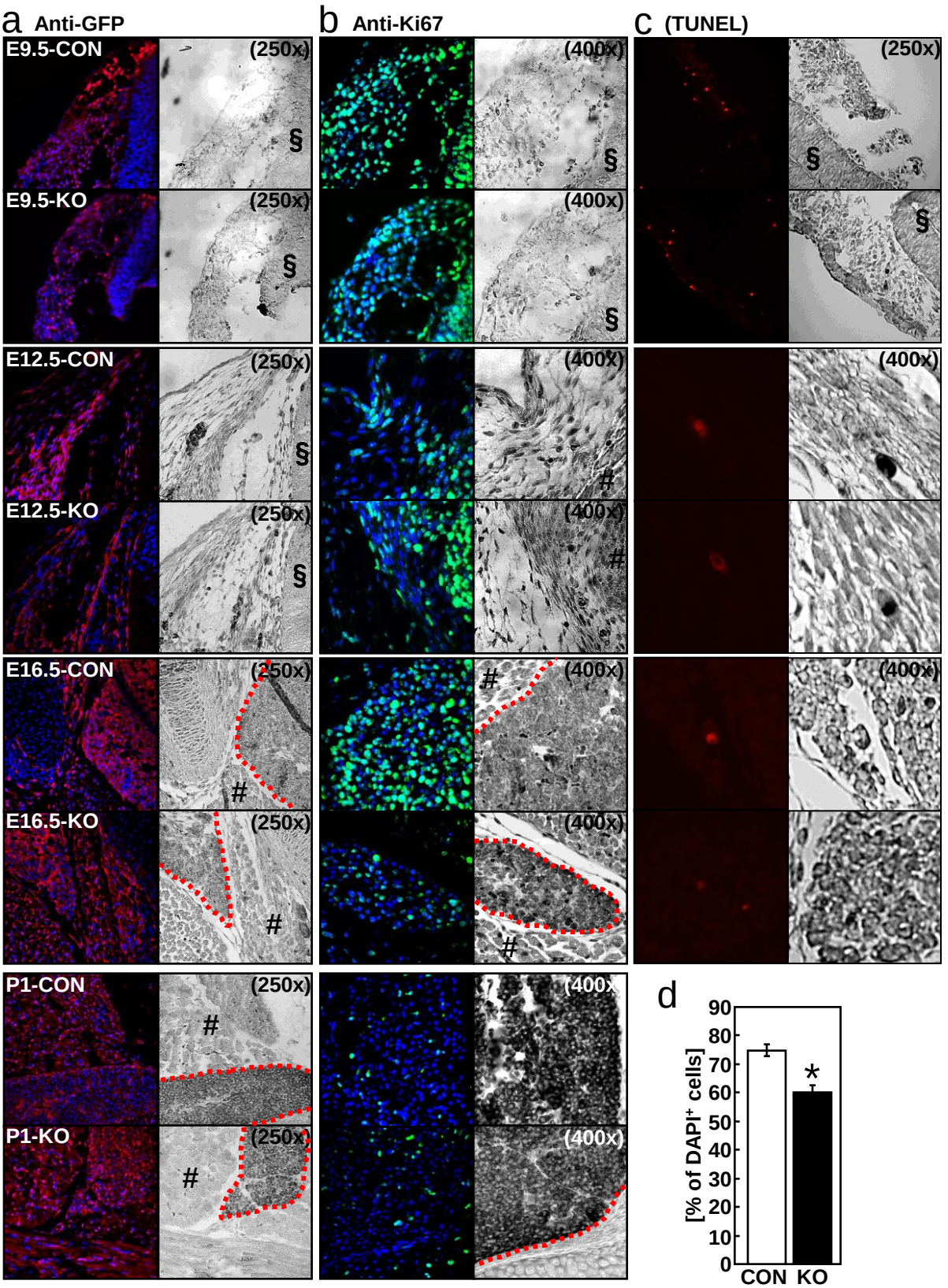

Supplementary Figure S2

Supplementary Figure S2

Loss of *Bmpr1a* results in decreased proliferation during embryonic expansion of cBAT, but does not affect cell death.

Myf5-Cre:R26YFP:BMPR1A double transgenic reporter animals were created by intercrossing the Myf5-Cre-mice with animals heterozygous for a Rosa26-YFP reporter and homozygous for the floxed *Bmpr1a* allele to allow for YFP-labelling of cells with presence of Cre-recombinase and therefore deletion of *Bmpr1a*. **a**, YFP-immunofluorescence (IF) (left panels, red) and DAPI, (blue) staining of control mice (CON) and Myf5-BMPR1A-KO (KO) mice at different developmental stages (E9.5, E12.5, E16.5 and P1). Second column of panels shows light microscopic images of the same area (applies to all panels of this figure; original magnification: 250x). § indicate location of the (YFP-negative) spinal cord, # indicate location of skeletal muscle bundles, and dotted lines surround the borders of brown fat pads (applies to all panels). Transversal sections of the same anatomical location were prepared for all developmental stages. **b**, Ki67-IF of same stages as indicated in panel a. Green indicates $Ki67^+$ nuclei and blue indicates DAPI-stained nuclei (original magnification: 400x). **c**, TUNEL-staining of same stages as indicated in panel a (except P1). Apoptotic nuclei are labelled in red, light microscopic image of same area are shown in right column of panels. **d**, Quantification of $Ki67^+$ nuclei in developing brown fat of E16.5 embryos. Quantification was done by counting total number $Ki67^+$ nuclei, not quantifying intensity of the staining, and normalizing to total number of $DAPI^+$ nuclei in two random photographs of cBAT-sections (control: n = 5; KO: n = 4). All data are presented as mean ± s.e.m. Asterisks denote significant differences between genotypes: * $P < 0.05$.

Discussion. To label cells with Myf5-Cre driven deletion of *Bmpr1a* during embryonic development, we intercrossed the Myf5-BMPR1A-KO mice with ROSA26-YFP-reporter mice. No changes in morphology were observed in embryonic stages prior to E16.5. This pertains to morphological analysis (H&E staining), proliferation (Ki67 staining), and cell death (TUNEL staining). At E16.5, the developing cBAT in wild-type control mice shows a marked increase of Ki67 staining when compared to other surrounding tissues, such as the spinal cord, developing muscle bundles, and osteogenic cells. While these findings do not rule out the possibility of an onset of increased proliferation at stages prior to E16.5, lack of a decisive cBAT-lineage marker labelling these earlier stages precludes a more detailed analysis. Since we observed no changes in cell death at any developmental stage, but a marked decrease of $Ki67^+$ nuclei at E16.5 in Myf5-BMPR1A-KO mice, we conclude that impairment of the rapid expansion of committed brown adipogenic progenitors in KO-mice contributes to the reduced size of cBAT after birth.

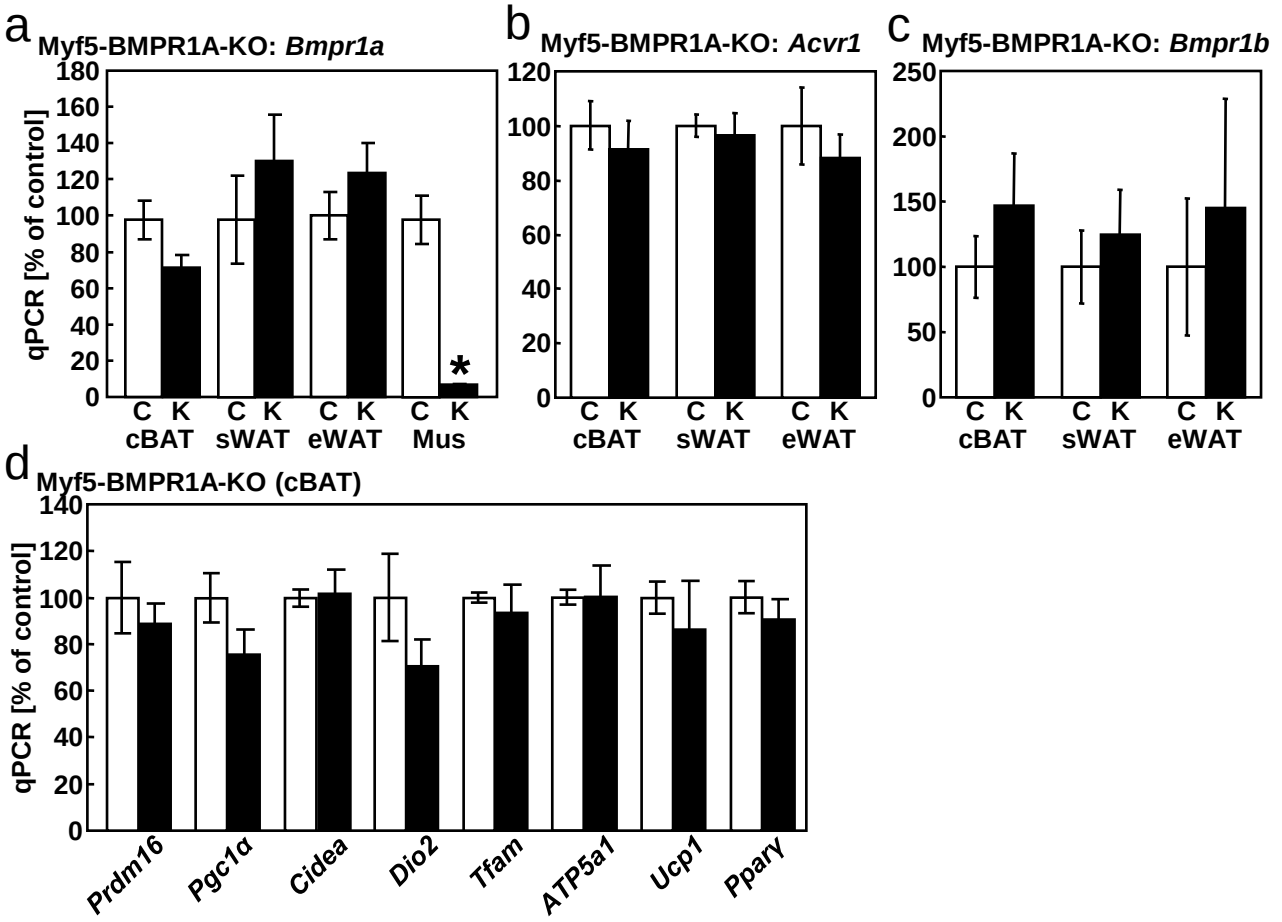

Supplementary Figure S3

Supplementary Figure S3

Residual brown adipose tissue in Myf5-BMPR1A-KO mice displays normal gene expression patterns and morphology.

a, qPCR of *Bmpr1a* mRNA in cBAT, sWAT, eWAT, and skeletal muscle (MUS) of adult Myf5-BMPR1A-KO animals (n = 3). White bars indicate littermate controls, black bars indicate Myf5-BMPR1A-KO mice (applies to all panels of this figure). **b**, **c**, qPCR analysis of type-I BMP receptors *Acvr1* (**b**) and *Bmpr1b* (**c**) mRNA in cBAT, sWAT, and eWAT (n = 4). **d**, qPCR analysis of mRNA of *Prdm16*, Peroxisome proliferator-activated receptor-γ coactivator 1 (*Pgc1*)-α, *Cidea*, Type II iodothyronine deiodinase (*Dio2*), mitochondrial Transcription factor A (*Tfam*), mitochondrial F1 complex ATP-synthase alpha subunit 1 (ATPase: *ATP5a1*), *Ucp1*, and *Pparγ* in cBAT of Myf5-BMPR1A-KO mice and littermate controls. All data are presented as mean ± s.e.m. (n = 3). **e**, H&E staining of cBAT from control (left panel) and Myf5-BMPR1A-KO mice (right panel). Tissue samples were paraffin-embedded and 6 µm sections were prepared and de-paraffinized before hematoxylin and eosin stainings (H&E staining) were performed. All data are presented as mean ± s.e.m. Asterisks indicate significant differences between genotypes: * $P < 0.05$.

Discussion. Gene expression analysis of the residual cBAT in control and KO animals did not reveal obvious changes, with the exception of a moderate decrease of *Bmpr1a* gene expression. These data suggest that the residual cBAT of KO mice may arise from incomplete recombination of Myf5-Cre or from a very small subset of cells derived from a Myf5^{-} lineage[18]. Histological analysis revealed no morphological changes, indicating that the residual brown adipocytes have normal fat content and do not represent a large number of undifferentiated progenitors that have not yet accumulated lipid. Moreover, expression of the other type 1 BMP-receptors, *Acvr1* and *Bmpr1b*, is not altered, suggesting that there is no compensation of BMP-signalling through increased expression of other BMP-receptors in the residual fat pad.

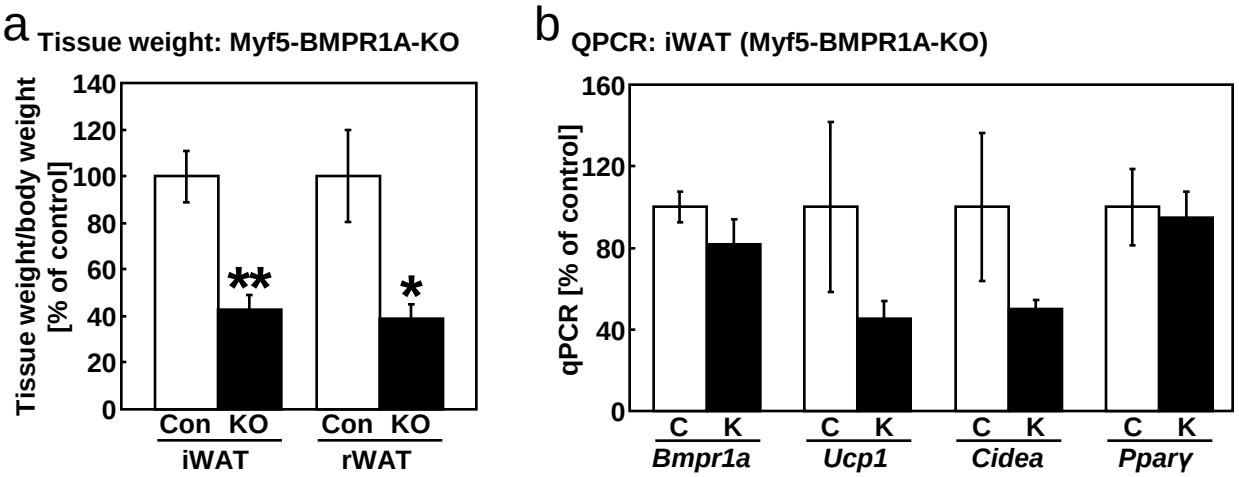

Supplementary Figure S4

Loss of *Bmpr1a* in Myf5$^+$ white adipose tissue results in decreased tissue size and reduction in BAT- but not WAT-gene expression.

a, Tissue weights of iWAT and rWAT normalized to body weight. White bars indicate littermate controls, black bars indicate Myf5-BMPR1A-KO mice (applies to all panels of this figure). **b**, qPCR analysis of *Bmpr1a*, *Ucp1*, *Cidea*, and *Pparγ* gene expression in iWAT. All data are presented as mean ± s.e.m. (control: n = 6; KO: n = 4). Asterisks denote significant differences between genotypes: * $P < 0.05$; ** $P < 0.01$.

Discussion. It has recently become clear that some of the minor white fat depots, particularly the interscapular and retroperitoneal white fat (iWAT and rWAT), are partially derived from a Myf5$^+$ lineage[18]. We therefore assessed the size of these white fat depots, and indeed observed a decreased size even after body weight normalization. Interestingly, expression of typical brow fat markers, such as *Ucp1* and *Cidea*, tended to be decreased, whereas general white adipogenic markers, such as *Pparγ*, were unchanged. Together, these findings indicate that loss of *Bmpr1a* also affects the browning of these other rBAT depots. Likewise, expression of *Bmpr1a* was not changed, indicating that deletion of *Bmpr1a* results in a loss of Myf5$^+$ cells that contribute to decreased tissue size in Myf5-BMPR1A-KO mice and the remaining iWAT or rWAT may be derived from the Myf5$^-$ progenitors. These findings also suggest that loss of the Myf5$^+$ progenitors preferentially affects brown adipogenesis. At the same time, compensatory browning of Myf5$^-$ adipocytes could partially restore brown adipocyte levels. However, due to the lack of available lineage markers for recruited brown adipocytes, it is currently not possible to assess to what extent rBAT derives from either Myf5$^+$ or Myf5$^-$ progenitors in these tissues.

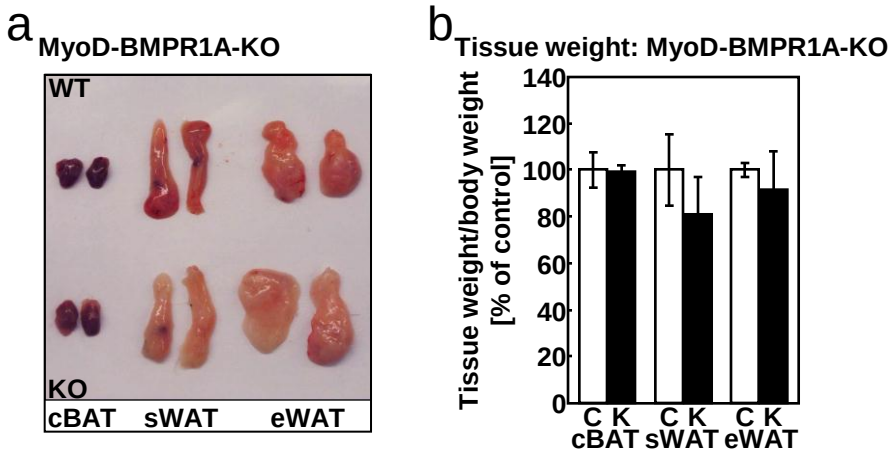

Supplementary Figure S5

Loss of *Bmpr1a* in the MyoD$^+$ lineage does not impair development of cBAT.

MyoD-BMPR1A-KO mice were created by intercrossing the MyoD-Cre-mice with animals carrying a floxed allele of *Bmpr1a*. **a**, **b**, Analysis of tissue weights from control and MyoD-BMPR1A-KO mice. All tissue weights were normalized to body weight for statistical analysis (**b**). All data are presented as mean ± s.e.m. (n = 3). White bars indicate littermate control animals and black bars indicate MyoD-BMPR1A-KO mice.

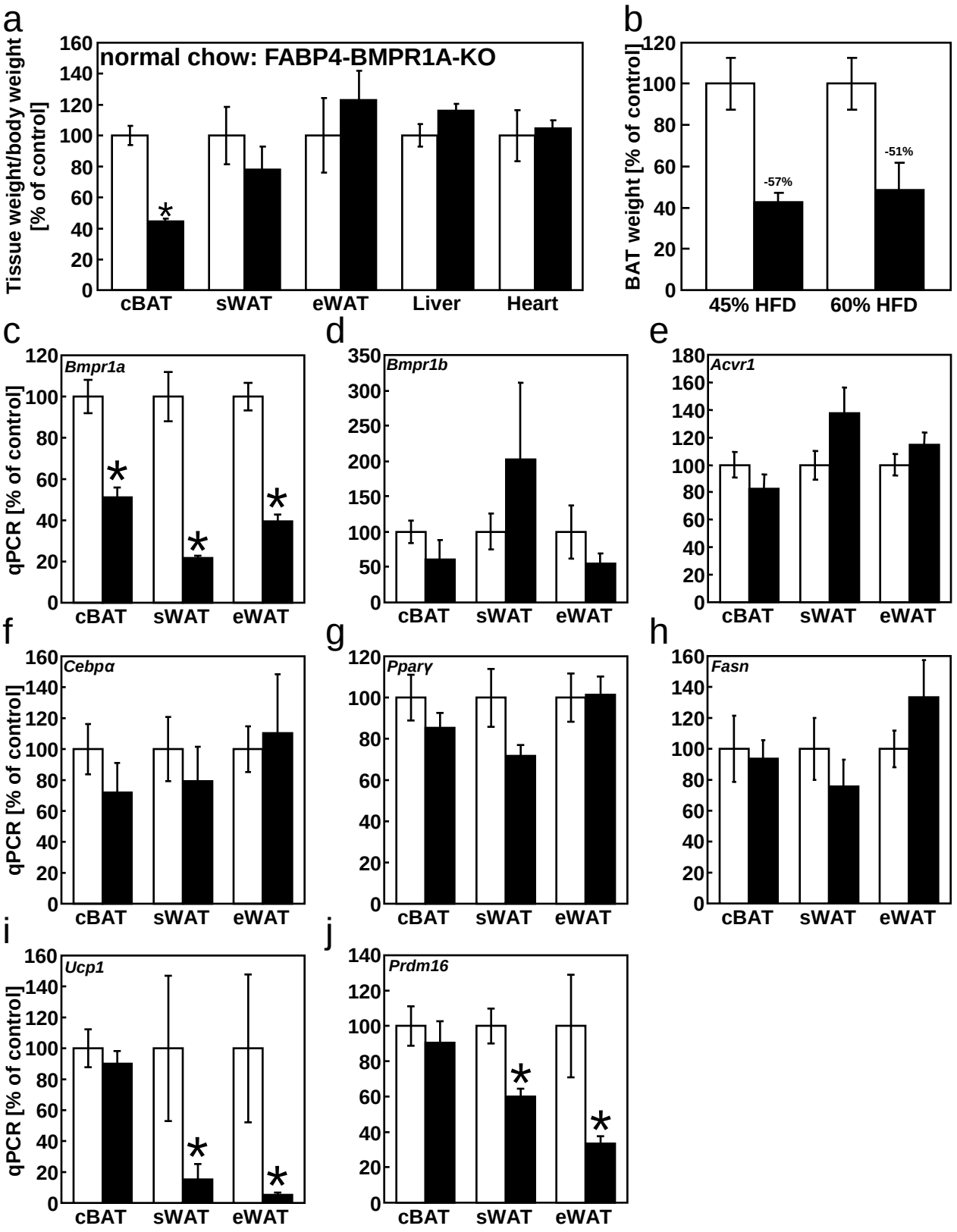

Supplementary Figure S6

Supplementary Figure S6

Loss of *Bmpr1a* in adipocytes specifically impairs formation and maintenance of brown, but not white, adipocytes.

FABP4-BMPR1A-KO mice were created by intercrossing the FABP4-Cre-mice with *Bmpr1a*-floxed mice. **a**, Tissue weight of brown and white fat pads from FABP4-BMPR1A-KO mice. All tissues were normalized to body weight for analysis (n = 4). White bars indicate control animals, black bars indicate FABP4-BMPR1A-KO mice (applies to all subsequent panels of this figure). **b**, Reduction of brown adipose depot weight in FABP4-BMPR1A-KO mice even after high fat feeding. Two different types of high fat diet were used: one contains 45% of calories from fat, and the other contains 60% from fat. (n = 4). **c**, **d**, **e**, qPCR analysis of type 1 BMP-receptors *Bmpr1a* (**c**), *Bmpr1b* (**d**), and *Acvr1* (**e**) mRNA in cBAT and white fat (sWAT and eWAT) of FABP4-BMPR1A-KO mice (n = 8). **f**, **g**, **h**, qPCR analysis of general adipogenic gene expression of *Cebpα* (**f**), *Pparγ* (**g**), and Fatty acid synthase (*Fasn*; **h**) in different fat depots of FABP4-BMPR1A-KO mice (n = 8). **i**, **j**, qPCR analysis of mRNA of brown adipocyte genes *Ucp1* (**i**) and *Prdm16* (**j**) in different fat depots of FABP4-BMPR1A-KO mice (n = 8). All data were repeated at least three times in different cohorts with comparable results. All data are presented as mean ± s.e.m. Asterisks denote significant differences between genotypes: * $P < 0.05$.

Discussion. While Myf5-driven Cre is turned on during early steps of embryogenesis, i.e. at the progenitor cell level, the FABP4-driven Cre is active in later stages of adipogenesis, and therefore affects differentiation of both brown and white adipocytes. Accordingly, expression of *Bmpr1a* was found to be significantly reduced in all fat depots tested. This general loss of BMPR1A in adipocytes decreases the size of cBAT, while the overall size of sWAT and eWAT was not affected. Importantly, FABP4-BMPR1A-KO mice displayed significant reduction in expression of BAT-markers in WAT, which serves as a measure of the decreased abundance of rBAT within the white fat, indicating that BMPR1A is critical for the formation of both types of brown fat, cBAT and rBAT. Along these lines, our findings suggest that BMP-signalling through BMPR1A might either be less critical for the formation of white adipocytes, or other type 1 receptors that are also expressed in WAT may compensate better for loss of BMPR1A in white adipocytes.

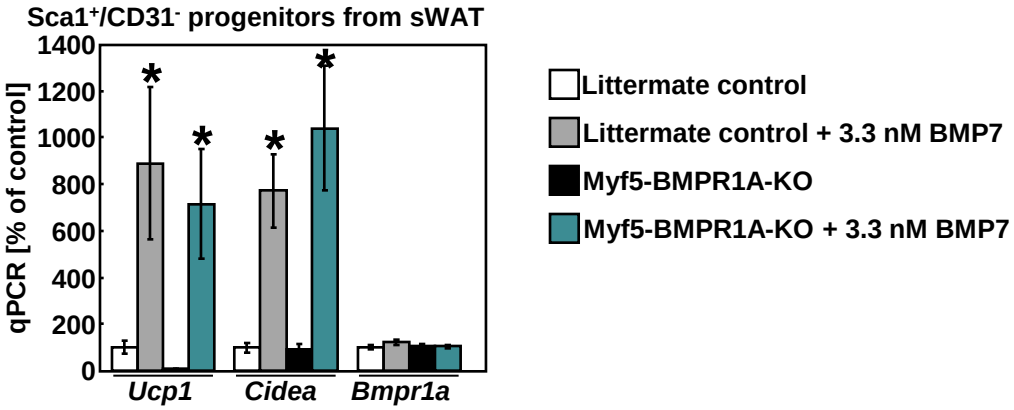

Supplementary Figure S7

Loss of *Bmpr1a* in the Myf5^{+} lineage does not affect brown adipogenic progenitors isolated from Myf5^{-} sWAT.

qPCR analysis of mRNA-levels of *Ucp1*, *Cidea*, and *Bmpr1a* in differentiated Sca1^{+} progenitors. Cells were isolated from sWAT of control mice and differentiated under basal conditions (white bars), with prior exposure to BMP7 for 3 days (grey bars), or from sWAT of Myf5-BMPR1A-KO mice treated with vehicle (black bars), or 3 days of BMP7 pre-treatment (blue bars) (n = 3). Experiment was repeated once with similar results. Data are presented as mean ± s.e.m. Asterisks denote significant differences between genotypes: * $P < 0.05$.

Discussion. While loss of *Bmpr1a* in the Myf5^{+} lineage that gives rise to cBAT reduces frequency of progenitor cells and their ability to differentiate (see Figure 2 of main text), no such impairment was observed in cells isolated form sWAT. These data are consistent with the notion that the majority of sWAT is derived from a Myf5^{-} lineage, and indicate that the Sca1^{+} progenitors isolated from sWAT retain full brown adipogenic capacity in response to BMP7 stimulation.

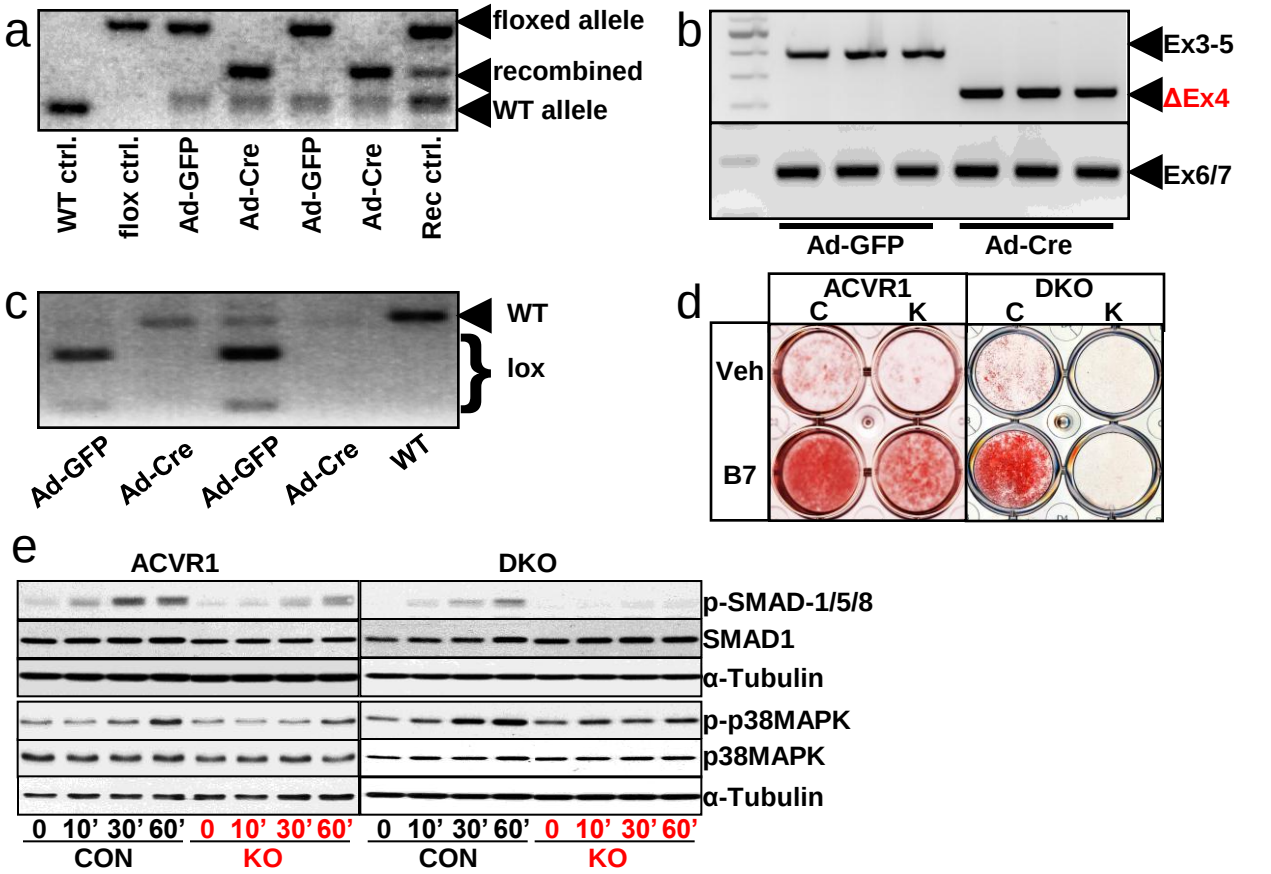

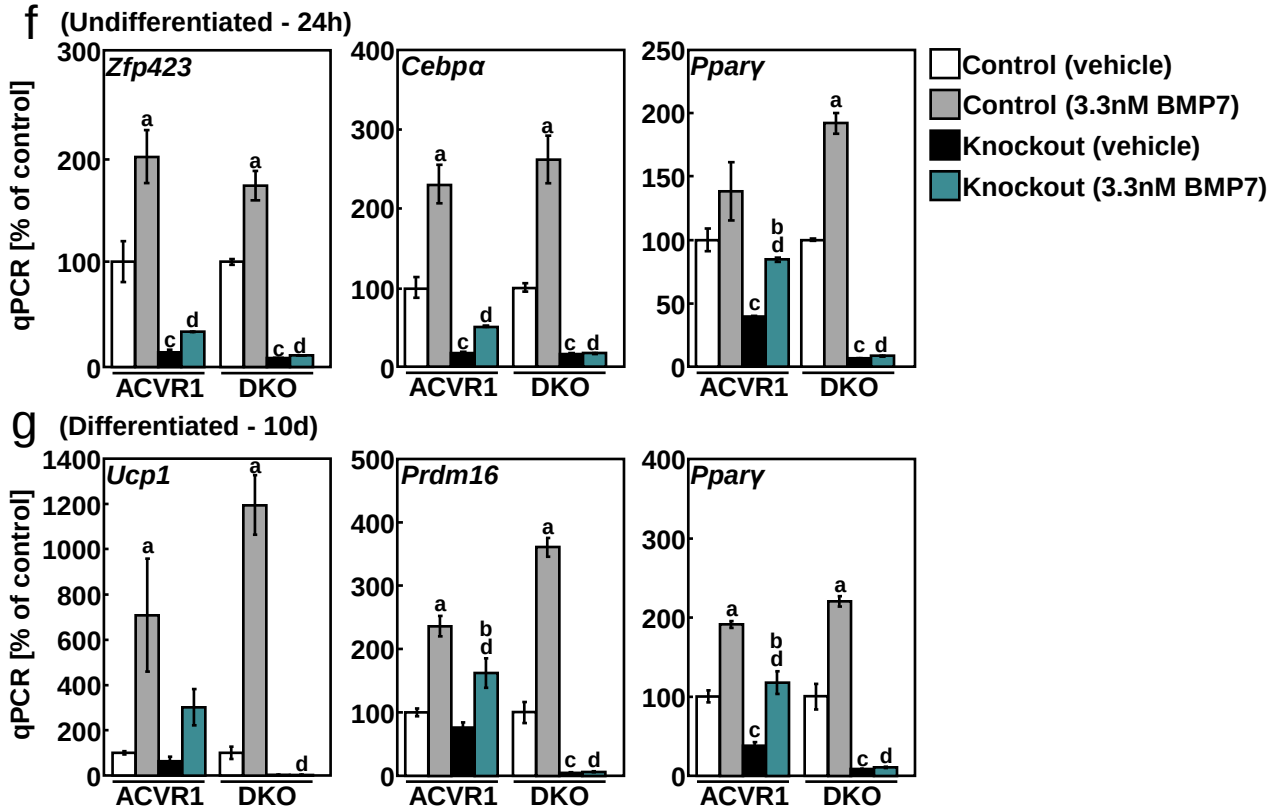

Supplementary Figure S8

Supplementary Figure S8

Loss of type 1 BMP-receptors ACVR1 and BMPR1A inhibits differentiation of brown adipocyte progenitor cells.

a, Cre-mediated DNA-recombination of the *Bmpr1a* gene in immortalized brown pre-adipocyte cell lines after infection with adenovirus expressing either GFP (Ad-GFP) or a Cre::GFP fusion protein (Ad-Cre) and subsequent FACS-purification of GFP^+ cells. **b**, PCR-amplification of recombined cDNA using primers annealing in exons 3 and 5, thus amplifying full length cDNA of immortalized brown pre-adipocyte cell lines between the two primers, or cDNA lacking exon 4 (ΔEx4, upper panel). Control primers annealing in exons 6 and 7 were used to amplify an intact portion of the cDNA as loading control (lower panel). Shown are triplicates from the same experiment. **c**, PCR amplifying unrecombined (Ad-GFP) or recombined (Ad-Cre) alleles of the floxed *Acvr1* gene locus in immortalized brown pre-adipocyte cell lines to show complete gene loss after virus infection and FACS-purification. Shown are duplicates from the same experiment. Band running slightly lower than WT band seen in some lanes is an unspecific amplification band. Loss of all three specific bands indicated gene loss following Cre recombination. **d**, Triglyceride-specific Oil Red O staining of differentiated control (C) pre-adipocytes or pre-adipocytes deficient for the BMP-receptor (K) ACVR1 (left panel), or BMPR1A and ACVR1 together (right panel; double knockout; DKO). Cell lines were pre-treated with 3.3 nM BMP7 (B7) of vehicle (Veh) for three days prior to differentiation. **e**, Western blot analysis of protein levels of phospho(p)-Smad1/5/8 (1^{st} row), basal Smad1 (2^{nd} row), corresponding α-Tubulin levels (3^{rd} row), phospho(p)-p38 mitogen activated protein kinase (p38; 4^{th} row), basal p38 (5^{th} row), and corresponding α-Tubulin levels (6^{th} row) in undifferentiated control (CON) and knock-out (KO) pre-adipocytes lacking either ACVR1 alone, or ACVR1 and BMPR1A together (DKO) following exposure to BMP7 for 10, 30, and 60 minutes. Each experiment was repeated two times, representative blots are shown. **f**, qPCR analysis of gene expression of *Zfp423*, *Cebpα*, and *Pparγ* in undifferentiated brown pre-adipocytes after 24h of exposure to BMP7. White bars indicate control cells, grey bars indicate control cells pre-treated with BMP7, black bars indicate knock-out cells, blue bars indicate knock-out cells treated with BMP7. Experiments depict results from cells lacking either ACVR1 alone, or both BMPR1A and ACVR1 (DKO). Statistically significant differences as determined by ANOVA ($p < 0.05$) were [a]control (vehicle) vs. control (+BMP7); [b]KO (veh) vs. KO (BMP7); [c]control (veh) vs. KO (veh); and [d]control (+BMP7) vs. KO (+BMP7). Applies to all subsequent panels. **g**, qPCR analysis of *Ucp1*, *Prdm16*, and *Pparγ* mRNA isolated from mature brown adipocytes following BMP7-pre-treatment and adipogenic differentiation for a total of 10 days. All qPCR-experiments (panels f and g) were performed twice with similar results. All data are presented as mean ± s.e.m.

Supplementary Figure S8 (continued)

Discussion. While deletion of *Bmpr1a* severely inhibits differentiation of brown pre-adipocytes, it does not completely block this process. We have therefore sought to determine whether other receptors might partially compensate for this process. To do this, we also generated cell lines with either a deletion of the type 1 receptor *Acvr1*, or both type 1 receptors, *Acvr1* and *Bmpr1a* (double knock-out, DKO). While ACVR1-deficient cells display a similar, albeit milder, phenotype compared to cells lacking BMPR1A, the DKO cells display complete blockage of differentiation and ability to respond to brown adipogenic stimuli such as BMP7-treatment. We therefore conclude, in combination with data from the mouse models described in Main Figure 2 and Supplementary Figure 9, that BMPR1A and ACVR1 are required for mediating the brown adipogenic effects of BMP-signalling, and that they may compensate for each other to some extent. Nevertheless, BMPR1A appears to be the major type 1 receptor controlling brown fat formation.

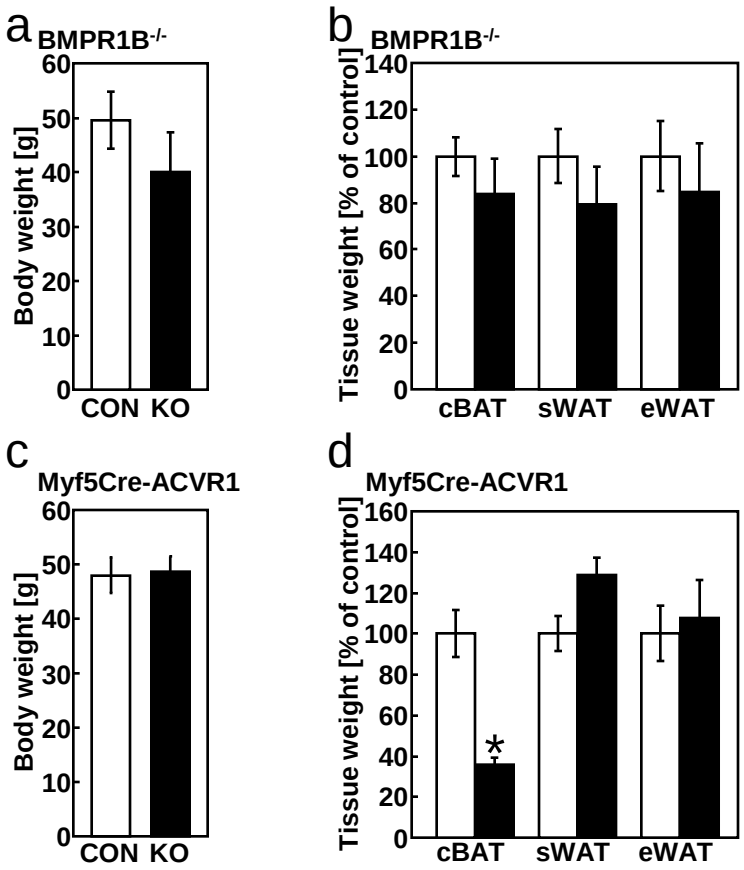

Supplementary Figure 9

Loss of type 1 BMP-receptors *Acvr1* and *Bmpr1a*, but not *Bmpr1b*, impairs cBAT-development.

a, Analysis of body weight of *Bmpr1b*-wholebody knockout mice (BMPR1B$^{-/-}$; control: n = 8; KO: n = 6). White bar indicates littermate controls and black bar indicates BMPR1B$^{-/-}$ (also applies to panel b). **b**, Tissue weights in cBAT and white fat depots (sWAT, eWAT) of BMPR1B$^{-/-}$ mice (control: n = 8; KO: n = 6). **c**, Analysis of body weight of Myf5-*ACVR1*-KO mice (control: n = 7; KO: n = 6). To generate these mice, Myf5-Cre mice were intercrossed with a strain of mice carrying a floxed allele for *Acvr1*. White bar indicates littermate controls and black bar indicates Myf5-ACVR1-KO mice (also applies to panel d). **d**, Tissue weights in brown (cBAT) and white fat depots (sWAT, eWAT) of Myf5-ACVR1-KO mice (control: n = 7; KO: n = 6). All data are presented as mean ± s.e.m. Asterisks denote significant differences between genotypes: * $P < 0.05$.

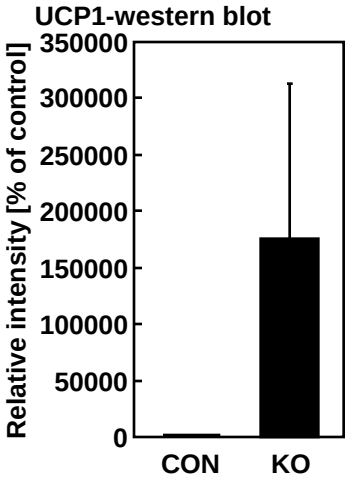

Supplementary Figure S10

Paucity of cBAT in Myf5-BMPR1A-KO mice results in increased UCP1 protein expression in sWAT under basal conditions.

Quantification of UCP1 protein expression in sWAT of Myf5-BMPR1A-KO mice by western blot (shown in Figure 3d). Bands for UCP1 and α-Tubulin (after re-probing of same membrane with appropriate antibody) were quantified using the program ImageJ. UCP1 band intensity was normalized to intensity of the corresponding tubulin band. White bar indicates control animals (n = 7; CON); black bar indicates knock-out mice (n = 7; KO). All data are presented as mean ± s.e.m.

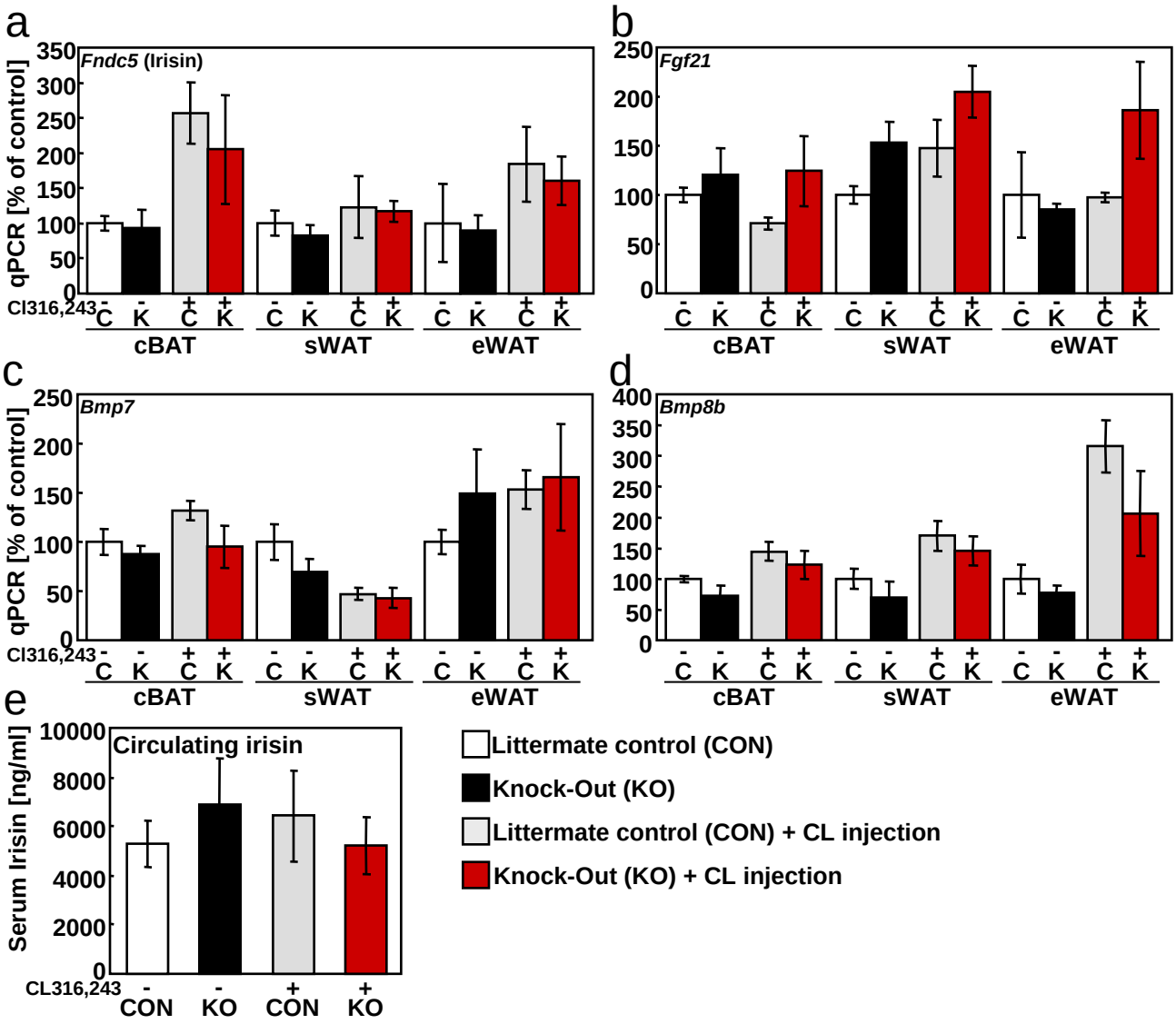

Supplementary Figure S11

Loss of cBAT does not result in increased expression of secreted browning factors.

a, **b**, **c**, **d**, qPCR analysis of recently identified browning molecules *Fndc5* (**a**; Irisin), *Fgf21* (**b**), *Bmp7* (**c**), and *Bmp8b* (**d**) in cBAT, sWAT, and eWAT. White bars (C) indicate control mice; black bars (K) indicate Myf5-BMPR1A-KO mice; grey bars indicate control animals after administration of β3-adrenergic agonist CL316,243 (1 mg/kg body weight, i.p.) for ten days; red bars indicate CL316,243-injected Myf5-BMPR1A-KO mice (n = 4). **e**, ELISA-Quantification of circulating irisin-levels (control: n = 9; KO: n = 8). All data are presented as mean ± s.e.m.

Discussion. Quantification of gene expression of some of the recently identified molecules that mediate browning through direct action on white adipose tissue did not reveal any differences, suggesting that these secreted signals may not be involved in the compensatory browning following loss of cBAT. Altogether these findings further support the hypothesis that direct sympathetic input to white adipose tissue might mediate these effects.

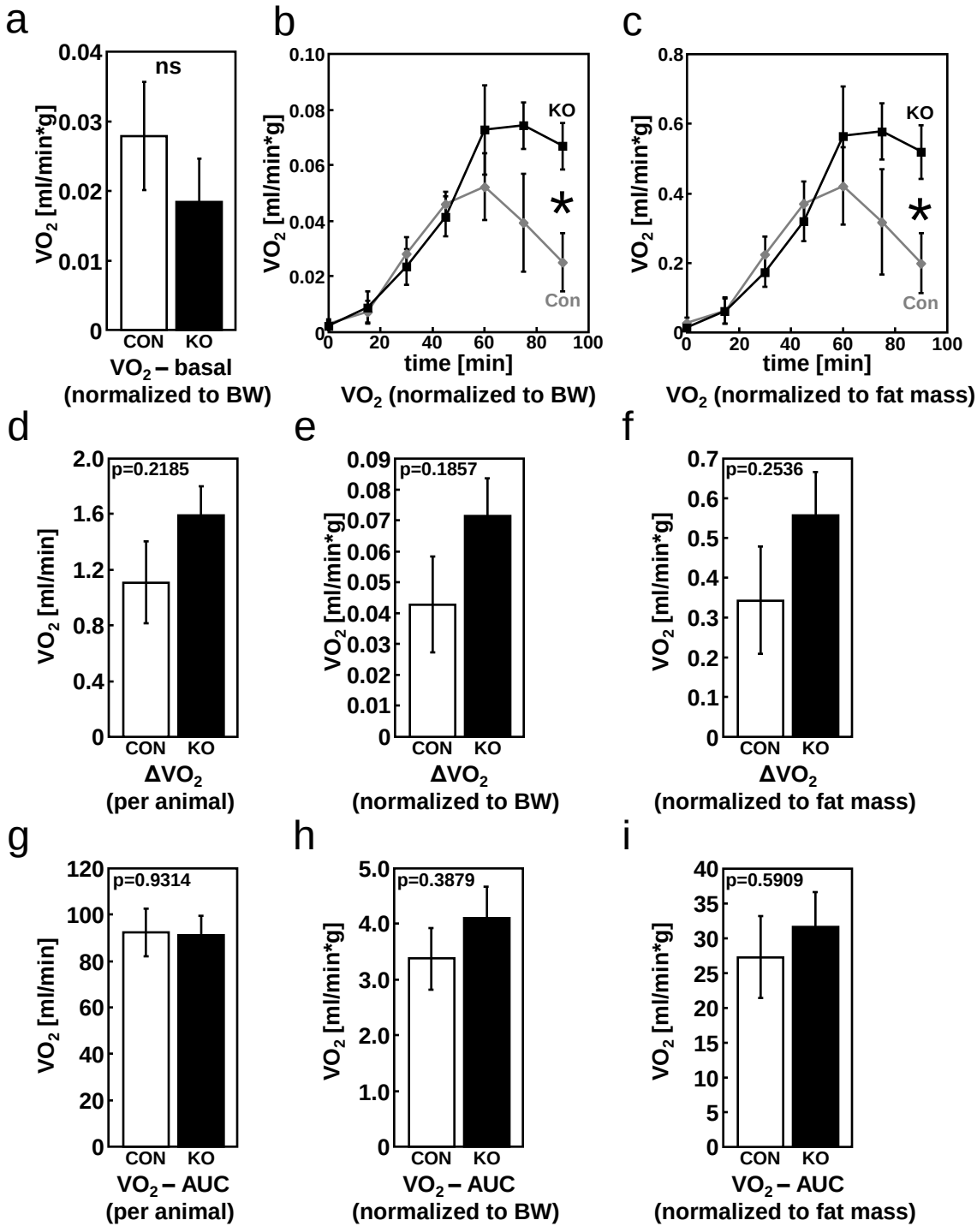

Supplementary Figure S12

Supplementary Figure S12

Compensatory browning of white fat results in normalization of thermogenic capacity in Myf5-BMPR1A-KO mice.

a, Basal average oxygen consumption (OC) prior to injection of noradrenaline (NA). Mice were maintained at 5° C for 8 days prior to experiment (control - white bars or grey lines; KO - black bars or lines; n = 5; Colour coding applies to all panels of this figure). Basal OC values were recorded for 30 min before NA-injections. The averages were then normalized to body weight (BW) to correct for the lower BW of Myf5-BMPR1A-KO mice. **b**, Time course of NA-induced OC after correction with basal OC and normalized to body weight (BW). **c**, Time course as described in panel b with the exception that OC was also normalized to total body fat content quantified by Dual Energy X-ray Absorptiometry (DEXA). **d**, **e**, **f**, Comparison and statistical analysis of maximum thermogenic capacity comparing absolute differences between basal OC and maximum NA-induced OC (ΔVO_2) in controls and Myf5-BMPR1A-KO mice. OC is expressed per animal (**d**), normalized to body weight (**e**), or normalized to fat mass (**f**). **g**, **h**, **i**, Comparison and statistical comparison of areas under the curve (AUC) for NA-induced OC per animal (**g**), normalized to body weight (**h**), or normalized to fat mass (**i**). All values are presented as mean ± s.e.m. (n = 5).

Discussion. In support of the findings depicted in Figure 3n, where the time course of oxygen consumption per animal is displayed, here we show different ways to normalize the raw data to show that the effects we observe are independent of the different body weights of both genotypes. Additionally, we have determined maximum differences in NA-induced oxygen consumption, i.e. ΔVO_2, and areas under the curves (AUC) for both genotypes and for all three ways of normalization. In both ΔVO_2 and AUC, no significant differences were observed between the genotypes, suggesting that the compensatory browning of white fat does indeed allow recovery and, importantly, full normalization of thermogenic capacity in the KO-mice with severe paucity of the cBAT depots. Taken together, these data suggest that compensatory browning in mice with severe cBAT paucity restores whole body thermogenic capacity to normal levels without producing unphysiological over-compensation.

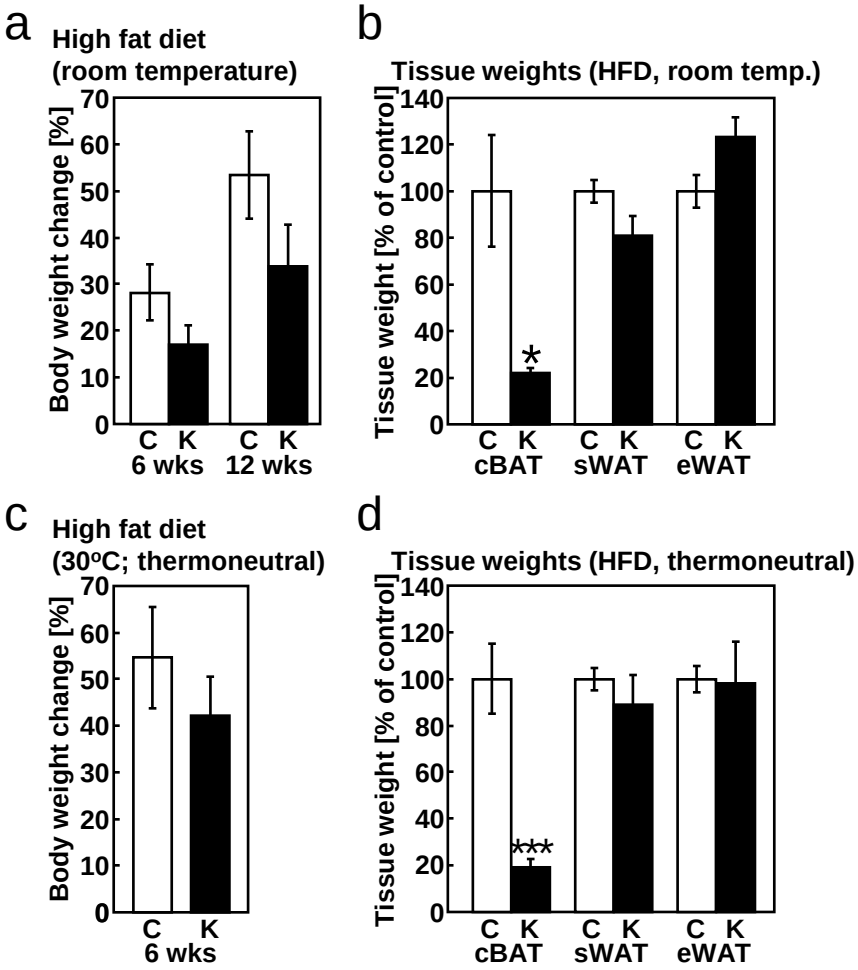

Supplementary Figure S13

Paucity of cBAT in Myf5-BMPR1A-KO mice does not result in increased susceptibility to diet-induced obesity under normal and thermoneutral conditions.

a, Analysis of body weight gain of Myf5-BMPR1A-KO mice after 6 and 12 weeks of high fat diet feeding. Body weight gain is expressed as percent increase of body weight from start of high fat diet feeding compared to the indicated time point (n = 3). **b**, Tissue weights of cBAT, sWAT, and eWAT in Myf5-BMPR1A-KO mice after high fat diet feeding (n = 3). **c**, Analysis of body weight gain of Myf5-BMPR1A-KO mice after 6 weeks of high fat diet feeding under thermoneutral conditions (n = 4). For thermoneutrality, mice were housed at 30 ºC for six weeks. **d**, Analysis of tissue weights of cBAT, sWAT, and eWAT of Myf5-BMPR1A-KO mice after six weeks of high fat diet feeding under thermoneutral conditions (n = 4). All data are presented as mean ± s.e.m. Asterisks denote significant differences between genotypes: * $P < 0.05$; ** $P < 0.01$; *** $P < 0.001$.

Supplementary Table 1: Primer-sequences used for QPCR analysis of gene expression.

Gene		Sequences
QPCR:		
Arbp (36B4)	Forward	TTTGGGCATCACCACGAAAA
	Reverse	GGACACCCTCCAGAAAGCGA
Acvr1 (Alk2)	Forward	TGCTAATGATGATGGCTTTCC
	Reverse	TTCACAGTGGTCCTCGTTCC
ATP5a1	Forward	TCTCCATGCCTCTAACACTCG
	Reverse	CCAGGTCAACAGACGTGTCAG
Bmp7	Forward	GGGCTTACAGCTCTCTGTGG
	Reverse	TGAAGGGTTGCTTGTTCTGG
Bmp8b	Forward	CCTCACTTGGACCGTGCT
	Reverse	CAGGGATCTGGGTTAGGTCA
Bmpr1A (Alk3)	Forward	CAGCAGGACCAGTCATTCAA
	Reverse	CTGGCTTCTTCTGGTCCAAG
Bmpr1B (Alk6)	Forward	CCCCACTCTGCCTCCTCT
	Reverse	GGTCGGGCTTCTTGTCTTTT
Cebpα	Forward	CAAGAACAGCAACGAGTACCG
	Reverse	GTCACTGGTCAACTCCAGCAC
Cidea	Forward	ATCACAACTGGCCTGGTTACG
	Reverse	TACTACCCGGTGTCCATTTCT
Dio2	Forward	CAGTGTGGTGCACTGCTCCAATC
	Reverse	TGAACCAAAGTTGACCACCAG
Fasn	Forward	GAGGACACTCAAGTGGCTGA
	Reverse	GTGAGGTTGCTGTCGTCTGT
Fgf21	Forward	GCTCTCTATGGATCGCCTCAC
	Reverse	GGTACACATTGTAACCGTCCTC
Fndc5[25]	Forward	ATGAAGGAGATGGGGAGGAA
	Reverse	GCGGCAGAAGAGAGCTATAACA
Pgc1α	Forward	CCCTGCCATTGTTAAGACC
	Reverse	TGCTGCTGTTCCTGTTTTC
Pparγ	Forward	TCAGCTCTGTGGACCTCTCC
	Reverse	ACCCTTGCATCCTTCACAAG
Prdm16	Forward	CAGCACGGTGAAGCCATTC
	Reverse	GCGTGCATCCGCTTGTG

Tfam	Forward	GTCCATAGGCACCGTATTGC
	Reverse	CCCATGCTGGAAAAACACTT
Ucp1	Forward	CTGCCAGGACAGTACCCAAG
	Reverse	TCAGCTGTTCAAAGCACACA
Zfp423	Forward	TGACGTTCGAGAACGAGAGA
	Reverse	GGGAGTCGAACATCTGGTTG
Genotyping		
Bmpr1a (cDNA)	Ex3_Forward	CCTCATTCACTTACACCAGTGAGAC
	Ex5_Reverse	CAGAGCCTTCATACTTCATACACCC
Bmpr1a (cDNA)	Ex6_Forward	CCAGCTACGCAGGACAATAGAAT
	Ex7_Reverse	GCAAAAGCAGCTGGAGAAGATGA
Bmpr1a (*Alk3*)	FX1	GGTTTGGATCTTAACCTTAGG
	FX2	GCAGCTGCTGCTGCAGCCTCC
	FX4	TGGCTACAATTTGTCTCATGC
Acvr1 (*Alk2*)	Forward	CCCCCATTGAAGGTTTAGAGAGAC
	Reverse	CTAAGAGCCATGACAGAGGTTG
Bmpr1b (*Alk6*)	ALK6-I	TGGTGAGTGGTTACAACAAGATCAGCA
	ALK6-E	CTCGGCCCAAGATCCTACGTTG
	NEO-Al2	GAAAGAACCAGCTGGGGCTCGAG
Rosa26-YFP	Common	AAAGTCGCTCTGAGTTGTTAT
	Wild type	GGAGCGGGAGAAATGGATATG
	Mutant	AAGACCGCGAAGAGTTTGTC
Myf5-Cre	Common-FWD	CGTAGACGCCTGAAGAAGGTCAACCA
	WT-REV	CACATTAGAAAACCTGCCAACACC
	MUT-REV	ACGAAGTTATTAGGTCCCTCGAC
Cre	Forward	CGTATATCCTGGCAGCGA
	Reverse	CCGTTTGCCGGTCGTGGG
IRS-1	Forward	ACAGCGTGAATTTTGGAGTCAGAA
	Reverse	GTCTTGCTCAGCCTCGCTAT

Supplementary Table 2: Analysis of gene expression levels.

Shown are average gene expression levels for all genes measured in this study. For general quality control, c_t-values were used when lower than 30, and melting curves for each primer pair were assessed to verify the quality of the amplicon prior to analysis.

Gene	sample type	c_t-value range
Acvr1	Brown adipose tissue	24
	Subcut. white adipose tissue	23
	Epididymal white adipose tissue	23
ATP5a1	Brown adipose tissue	15
Bmp7	Brown adipose tissue	28-29
	Subcut. white adipose tissue	26-27
	Epididymal white adipose tissue	26-27
Bmp8a	Brown adipose tissue	24
	Subcut. white adipose tissue	26-27
	Epididymal white adipose tissue	25-27
Bmpr1a	Brown adipose tissue	22-23
	Subcut. white adipose tissue	21-23
	Epididymal white adipose tissue	21-23
	Skeletal muscle	22-26
	Sca1+ primary pre-adipoctes (BAT)	21-22
	Sca1+ primary pre-adipoctes (sWAT)	22
Bmpr1b	Brown adipose tissue	28
	Subcut. white adipose tissue	30
	Epididymal white adipose tissue	30
Cebpα	Brown adipose tissue	20-21
	Subcut. white adipose tissue	20-21
	Epididymal white adipose tissue	20-21
	Immortalized brown pre-adipoctes	22-25
Cidea	Brown adipose tissue	15-16
	Subcut. white adipose tissue	17-21
	Epididymal white adipose tissue	19-24
	Sca1+ primary pre-adipoctes (BAT)	19-24
	Sca1+ primary pre-adipoctes (sWAT)	21-22
Dio2	Brown adipose tissue	23
Fasn	Brown adipose tissue	15
	Subcut. white adipose tissue	19
	Epididymal white adipose tissue	19
Fgf21	Brown adipose tissue	28-29
	Subcut. white adipose tissue	28-29
	Epididymal white adipose tissue	28-29
Fndc5	Brown adipose tissue	26
	Subcut. white adipose tissue	27-28
	Epididymal white adipose tissue	26-27
Pgc1α	Brown adipose tissue	22

Pparγ	Brown adipose tissue	19
	Subcut. white adipose tissue	20
	Epididymal white adipose tissue	20
	Immortalized brown pre-adipoctes	21- >30
Prdm16	Brown adipose tissue	24
	Subcut. white adipose tissue	25
	Epididymal white adipose tissue	26-28
	Immortalized brown pre-adipoctes	25-30
Tfam	Brown adipose tissue	22
Ucp1	Brown adipose tissue	13-14
	Subcut. white adipose tissue	17-23
	Epididymal white adipose tissue	19-28
	Sca1+ primary pre-adipoctes (BAT)	21-23
	Sca1+ primary pre-adipoctes (sWAT)	23-24
	Immortalized brown pre-adipoctes	21- >30
Zfp423	Immortalized brown pre-adipoctes	28-29